Wind and Wave Induced Currents in a Rotating Sea with Depth-varying Eddy Viscosity

ALASTAIR D. JENKINS

Oceanographic Center, The SINTEF Group, N-7034 Trondheim-NTH, Norway

(Manuscript received 24 June 1986, in final form 4 December 1986)

ABSTRACT

A theory is presented for time-dependent currents induced by a variable wind stress and wave field in deep water away from coastal boundaries. It is based on a second-order perturbation expansion of a version of the Navier-Stokes equations in Lagrangian coordinates. The Coriolis effect and the effect of a depth-dependent eddy viscosity are included. (The eddy viscosity is taken to depend on the Lagrangian vertical coordinate $\hat{c}$.) Partial differential equations are derived for the vertical and time variation of the mass transport velocity, together with boundary conditions at the sea surface. The vertical variation of the eddy viscosity causes an extra source term to appear in the equation for the evolution of the current profile. This additional source of momentum within the water column is exactly balanced by an extra term in the surface boundary condition, which in turn represents the contribution to wave dissipation caused by the eddy viscosity within the water column being different from its surface value.

The equations were solved numerically, using a constant wind stress and monochromatic wave field simultaneously applied in the same direction at time $\hat{t} = 0$. The eddy viscosity ν was assumed to be proportional to depth, using Madsen's relation ($\nu = -\kappa_K u_* \hat{c}$, where κ_K is von Kármán's constant, $u_* = (\hat{\tau}/\rho)^{1/2}$ where $\hat{\tau}$ is the wind stress and ρ is the water density), except for near the surface where it was modified to account empirically for the direct effects of breaking waves. Results for the Lagrangian mean current were in general agreement with observations: long-term average values ranged from 2.2% to 2.8% of the wind speed at the 10 m level, and were directed between 12° and 17° to the right of the wind and wave direction (in the Northern Hemisphere). The deviation of the current from the wind direction is closer to observed drift current observations than the corresponding results for a constant eddy viscosity. The Lagrangian mean current is surprisingly close to the current obtained from Madsen's theory, even though Madsen does not account explicitly for the effect of surface waves.

The theory can easily take account of random sea states. There are good prospects for coupling it with the output of a numerical model for surface gravity waves, using the wave model's input and dissipation source terms.

1. Introduction

The theory of the response of the near-surface current profile to pure wind forcing is quite well established, the details of the response depending principally upon the vertical variation of the eddy viscosity and density structure (e.g., see Ekman, 1902, 1905; Dobroklonskiy, 1969; Gonella, 1971; Lai and Rao, 1976; Madsen, 1977; Pollard, 1980). However, the effect of the wind in producing currents in the ocean is complicated considerably by the presence of wind-generated surface waves. Stokes (1847) showed that, to second order in the wave slope, in the absence of viscosity and rotation, the waves induce a drift current along the wave direction.

In the presence of the Earth's rotation, Ursell (1950) demonstrated that in an inviscid ocean a wave field could not in fact induce a net steady mass transport. The wave-induced horizontal motion then consists of inertial oscillations with a zero Lagrangian mean (Hasselmann, 1970; Pollard, 1970).

For wave-induced drift in the absence of rotation, Longuet-Higgins (1953, 1960) showed that the presence of even a small viscosity produces significant changes in the mass transport not only in thin boundary layers near the surface and bottom, but also in the interior of the fluid. His analysis involved solving the equations of motion in an Eulerian curvilinear coordinate system which was attached to the moving surface boundary. Chang (1969) and Ünlüata and Mei (1973) calculated the mass transport using Lagrangian coordinates, their treatments being based on Pierson's (1962) perturbation expansion of the Navier-Stokes equations.

Weber (1983a,b) used the Lagrangian coordinate perturbation expansion to derive (i) time-dependent results for mass transport due to a spatially uniform field of decaying swell in a deep rotating ocean with viscosity, the decay rate being determined by the value of the viscosity, and (ii) steady state results for mass transport due to a spatially uniform wind and wave field. Weber's theory was extended by Jenkins (1986, hereafter referred to as J1) to take account of more-or-less arbitrary temporal variations in the wind stress and wave field. This requires that the wave field be allowed to vary spatially, and it was found that such spatial and temporal variations could be handled in a self-consistent manner. In the limit of time $\hat{t} \to \infty$, Weber's (1983b) equations, surface boundary condi-

tion and vertical current profile were obtained. The inviscid results of Pollard (1970) and Hasselmann (1970), showing a zero net wave-induced mass transport with inertial oscillations superimposed, were approached when the eddy viscosity was made very small. The eddy viscosity was, however, still required to be constant.

An approximation to a generally accepted value for the surface wind-induced drift—roughly 3% of the wind speed, 10° to the right of the wind direction (Kirwan et al., 1979; J. C. Huang, 1983)—was obtained by the theory of Madsen (1977), which uses an eddy viscosity increasing linearly with depth and does not include wave effects. It should, however, be noted that widely varying figures for observed surface wind-induced drift have been reported in the literature (N. E. Huang, 1979). The effect of depth variation of the eddy viscosity on the behavior of the near-surface wind-induced current has also been investigated in numerical modelling studies (Davies, 1985a,b).

A realistic theory for wave-induced currents which makes use of the eddy viscosity concept should thus also allow the eddy viscosity to vary with depth, whereas the theory presented in Weber (1983a,b) and J1 requires the eddy viscosity to be constant. Johns (1970) considered the case of a spatially varying eddy viscosity within the bottom boundary layer. Barstow (1981) used the Lagrangian perturbation expansion technique to derive some equations for near-surface wave-induced drift in the presence of an eddy viscosity, which was dependent on the Eulerian vertical coordinate ($\hat{z}$) within the main body of the fluid. It is, however, more natural to assume that the eddy viscosity is a function of the Lagrangian vertical coordinate ($\hat{c}$); this can be illustrated by the following example.

In Fig. 1, both graphs show schematic time series of the surface elevation, and of the vertical position of a water particle at $\hat{z} = \hat{z}_1$ when the surface is at $\hat{z} = 0$. In the upper graph, the eddy viscosity is a function of the Eulerian vertical coordinate: it is equal to ν_1 when $\hat{z} > \hat{z}_2$ and is equal to ν_2 when $\hat{z} \leqslant \hat{z}_2$. In the lower graph, ν is a function of the Lagrangian vertical coordinate $\hat{c}$; $\nu = \nu_1$ for water particles which are above $\hat{c} = \hat{c}_2$ (those which are above $\hat{z} = \hat{z}_2$ when the surface is at $\hat{z} = 0$), and $\nu = \nu_2$ for water particles which are below $\hat{c} = \hat{c}_2$.

In the case where the eddy viscosity depends on the Lagrangian vertical coordinate, each water particle will remain in a region with the same eddy viscosity throughout the wave cycle. If the eddy viscosity depends on the Eulerian vertical coordinate, a water particle can be subject to different eddy viscosities in different parts of the wave cycle. For example, in Fig. 1, a water particle which is at $\hat{z}_1$ when the surface is at $\hat{z} = 0$ is subject to an eddy viscosity ν_2 when $\hat{t}_1 \leqslant \hat{t} \leqslant \hat{t}_4$, but is otherwise subject to an eddy viscosity ν_1. A water particle at the sea surface is subject to a change in eddy viscosity at $\hat{t}_2$ and $\hat{t}_3$.

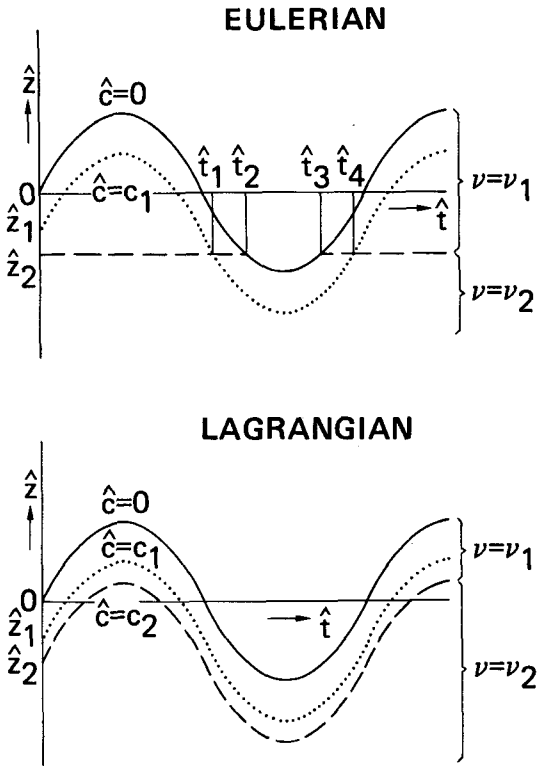

FIG. 1. Example illustrating the variation of eddy viscosity with Eulerian depth ($-\hat{z}$) and with Lagrangian depth ($-\hat{c}$).

The situation can, of course, be generalized to the case of a continuous variation of ν with either $\hat{c}$ or $\hat{z}$. Barstow (1981) treated the variation of $\hat{z}$-dependent ν through the wave cycle by performing a perturbation expansion of ν in powers of the wave slope. Such a perturbation expansion will be valid if the variation of ν following a water particle during a wave cycle is not too great, which means that ν should not vary too much with depth. This restriction on the vertical variation of ν does not apply if ν is just dependent on $\hat{c}$, since a water particle is always subject to the same eddy viscosity and a perturbation expansion for ν is not required. We thus use a purely $\hat{c}$-dependent eddy viscosity in this paper.

2. Mathematical formulation

The sea is considered to be a homogeneous incompressible viscous fluid of constant density ρ rotating counterclockwise about a vertical axis with an angular velocity $f/2$. A right-handed Cartesian coordinate system is chosen with the x_1- and x_2-axes along the undisturbed sea surface and the x_3-axis pointing vertically upwards. The sea is assumed to be so deep that surface gravity waves do not feel the bottom, and of such great horizontal extent that the boundaries do not affect the water motion in the area of interest.

We use the following form of the equations of motion:

$$\frac{D\hat{u}_i}{D\hat{t}} = -(\mathbf{f}\times\hat{\mathbf{u}})_i - g\delta_{i3} - \frac{1}{\rho}\frac{\partial \hat{p}}{\partial x_i} + \frac{\partial}{\partial x_j}\left[\nu\left(\frac{\partial \hat{u}_j}{\partial x_i} + \frac{\partial \hat{u}_i}{\partial x_j} - \frac{1}{3}\frac{\partial \hat{u}_k}{\partial x_k}\delta_{ij}\right)\right], \quad (2.1)$$

$$\frac{\partial \hat{u}_j}{\partial x_j} = 0, \quad (2.2)$$

where the $\hat{u}_i$ are the velocity components, $\hat{p}$ is the pressure, ν is a spatially variable kinematic eddy viscosity, $\mathbf{f} = (0, 0, f)$, g is the acceleration due to gravity, the subscripts i, j and k range from 1 to 3 and terms with repeated subscripts are summed over the range of the subscript. $(D/D\hat{t})$ represents the convective time derivative. We assume that the eddy viscosity acts in the same way as a hypothetical spatially varying Newtonian viscosity, so that the "viscous" shear stress is equal to the eddy viscosity multiplied by the symmetric traceless part of the rate-of-shear tensor.

Using the continuity equation (2.2), the momentum equation (2.1) becomes

$$\frac{D\hat{u}_i}{D\hat{t}} = -(\mathbf{f}\times\hat{\mathbf{u}})_i - g\delta_{i3} - \frac{1}{\rho}\frac{\partial \hat{p}}{\partial x_i} + \frac{\partial \nu}{\partial x_j}\left(\frac{\partial \hat{u}_j}{\partial x_i} + \frac{\partial \hat{u}_i}{\partial x_j}\right) + \nu\nabla^2\hat{u}_i. \quad (2.3)$$

We now convert the equations of motion (2.2) and (2.3) to equations in a Lagrangian coordinate system. The fluid particles are labeled with the Lagrangian coordinates $(\hat{a}, \hat{b}, \hat{c})$, the undisturbed state being

$$\hat{x} \equiv x_1 = \hat{a}, \quad \hat{y} \equiv x_2 = \hat{b}, \quad \hat{z} \equiv x_3 = \hat{c}, \quad \hat{p} = \hat{p}_0 - \rho g\hat{c}, \quad (2.4)$$

where $\hat{p}_0$ is the atmospheric pressure. We obtain

$$\hat{x}_{\hat{t}\hat{t}} = f\hat{y}_{\hat{t}} - \frac{1}{\rho}\frac{\partial(\hat{p},\hat{y},\hat{z})}{\partial(\hat{a},\hat{b},\hat{c})} + 2\frac{\partial(\nu,\hat{y},\hat{z})}{\partial(\hat{a},\hat{b},\hat{c})}\frac{\partial(\hat{x}_{\hat{t}},\hat{y},\hat{z})}{\partial(\hat{a},\hat{b},\hat{c})} + \frac{\partial(\hat{x},\nu,\hat{z})}{\partial(\hat{a},\hat{b},\hat{c})}\left[\frac{\partial(\hat{y}_{\hat{t}},\hat{y},\hat{z})}{\partial(\hat{a},\hat{b},\hat{c})} + \frac{\partial(\hat{x},\hat{x}_{\hat{t}},\hat{z})}{\partial(\hat{a},\hat{b},\hat{c})}\right] + \frac{\partial(\hat{x},\hat{y},\nu)}{\partial(\hat{a},\hat{b},\hat{c})}\left[\frac{\partial(\hat{z}_{\hat{t}},\hat{y},\hat{z})}{\partial(\hat{a},\hat{b},\hat{c})} + \frac{\partial(\hat{x},\hat{y},\hat{x}_{\hat{t}})}{\partial(\hat{a},\hat{b},\hat{c})}\right] + \nu\nabla^2\hat{x}_{\hat{t}},$$

$$\hat{y}_{\hat{t}\hat{t}} = -f\hat{x}_{\hat{t}} - \frac{1}{\rho}\frac{\partial(\hat{x},\hat{p},\hat{z})}{\partial(\hat{a},\hat{b},\hat{c})} + \frac{\partial(\nu,\hat{y},\hat{z})}{\partial(\hat{a},\hat{b},\hat{c})}\left[\frac{\partial(\hat{x},\hat{x}_{\hat{t}},\hat{z})}{\partial(\hat{a},\hat{b},\hat{c})} + \frac{\partial(\hat{y}_{\hat{t}},\hat{y},\hat{z})}{\partial(\hat{a},\hat{b},\hat{c})}\right] + 2\frac{\partial(\hat{x},\nu,\hat{z})}{\partial(\hat{a},\hat{b},\hat{c})}\frac{\partial(\hat{x},\hat{y}_{\hat{t}},\hat{z})}{\partial(\hat{a},\hat{b},\hat{c})} + \frac{\partial(\hat{x},\hat{y},\nu)}{\partial(\hat{a},\hat{b},\hat{c})}\left[\frac{\partial(\hat{x},\hat{z}_{\hat{t}},\hat{z})}{\partial(\hat{a},\hat{b},\hat{c})} + \frac{\partial(\hat{x},\hat{y},\hat{y}_{\hat{t}})}{\partial(\hat{a},\hat{b},\hat{c})}\right] + \nu\nabla^2\hat{y}_{\hat{t}},$$

$$\hat{z}_{\hat{t}\hat{t}} = -g - \frac{1}{\rho}\frac{\partial(\hat{x},\hat{y},\hat{p})}{\partial(\hat{a},\hat{b},\hat{c})} + \frac{\partial(\nu,\hat{y},\hat{z})}{\partial(\hat{a},\hat{b},\hat{c})}\left[\frac{\partial(\hat{x},\hat{y},\hat{x}_{\hat{t}})}{\partial(\hat{a},\hat{b},\hat{c})} + \frac{\partial(\hat{z}_{\hat{t}},\hat{y},\hat{z})}{\partial(\hat{a},\hat{b},\hat{c})}\right] + \frac{\partial(\hat{x},\nu,\hat{z})}{\partial(\hat{a},\hat{b},\hat{c})}\left[\frac{\partial(\hat{x},\hat{y},\hat{y}_{\hat{t}})}{\partial(\hat{a},\hat{b},\hat{c})} + \frac{\partial(\hat{x},\hat{z}_{\hat{t}},\hat{z})}{\partial(\hat{a},\hat{b},\hat{c})}\right] + 2\frac{\partial(\hat{x},\hat{y},\nu)}{\partial(\hat{a},\hat{b},\hat{c})}\frac{\partial(\hat{x},\hat{y},\hat{z}_{\hat{t}})}{\partial(\hat{a},\hat{b},\hat{c})} + \nu\nabla^2\hat{z}_{\hat{t}}, \quad (2.5)$$

$$\frac{\partial(\hat{x},\hat{y},\hat{z})}{\partial(\hat{a},\hat{b},\hat{c})} = 1, \quad (2.6)$$

where the $\hat{t}$ subscript denotes differentiation with respect to time and $\partial(\cdot)/\partial(\cdot)$ is the Jacobian operator, i.e.

$$\frac{\partial(X,Y,Z)}{\partial(a,b,c)} \equiv \begin{vmatrix} \partial X/\partial a & \partial Y/\partial a & \partial Z/\partial a \\ \partial X/\partial b & \partial Y/\partial b & \partial Z/\partial b \\ \partial X/\partial c & \partial Y/\partial c & \partial Z/\partial c \end{vmatrix} \quad (2.7)$$

for any variables X, Y, Z, a, b, c.

The ∇^2 terms expressed in terms of Lagrangian coordinates are complicated expressions involving Jacobians of Jacobians, and are given explicitly by, for example, Pierson (1962).

Following Pierson, we expand the solution to Eqs. (2.5) and (2.6) in terms of a small parameter ϵ, which we will later take to be approximately equal to the wave slope near $\hat{a} = \hat{t} = 0$:

$$\hat{x} = \hat{a} + \epsilon\hat{x}^{(1)} + \epsilon^2\hat{x}^{(2)} + \cdots$$
$$\hat{y} = \hat{b} + \epsilon\hat{y}^{(1)} + \epsilon^2\hat{y}^{(2)} + \cdots$$
$$\hat{z} = \hat{c} + \epsilon\hat{z}^{(1)} + \epsilon^2\hat{z}^{(2)} + \cdots$$
$$\hat{p} = \hat{p}_0 - \rho g\hat{c} + \epsilon\hat{p}^{(1)} + \epsilon^2\hat{p}^{(2)} + \cdots. \quad (2.8)$$

The free surface is described by

$$\hat{\zeta} = \hat{z}\,(\hat{c} = 0) = \epsilon\hat{z}^{(1)} + \epsilon^2\hat{z}^{(2)} + \cdots(\hat{c} = 0). \quad (2.9)$$

The perturbation quantities $\hat{x}^{(1)}$, $\hat{x}^{(2)}$, $\hat{y}^{(1)}$ etc. are assumed to vanish as $\hat{c} \to -\infty$.

3. First-order equations

a. Derivation

To $O(\epsilon)$, we assume we have surface gravity waves with angular frequency σ propagating in the $\hat{x}$-direc-

tion. To this order the Earth's rotation (Coriolis effect) can be ignored. It can be shown that if the Coriolis effect is included, it gives rise just to a small periodic particle displacement along the wave crests which is $O(f/\sigma)$ times (roughly 10^{-4} times) the total periodic particle displacement. This in turn gives rise to a contribution to the Lagrangian mean $O(\epsilon^2)$ current, which is negligible in comparison to the contributions from other mechanisms, including the Coriolis effect on the Lagrangian mean $O(\epsilon^2)$ current itself (Weber, 1987).

We thus assume that the $O(\epsilon)$ velocity component in the $\hat{y}$-direction is negligible and that all derivatives in the $\hat{y}$-direction can be neglected. We introduce nondimensional coordinates and variables:

$$x=(\sigma^2/g)\hat{x},\quad y=(\sigma^2/g)\hat{y},\quad z=(\sigma^2/g)\hat{z},$$
$$p=(\sigma^2/\rho g^2)\hat{p}$$
$$a=(\sigma^2/g)\hat{a},\quad b=(\sigma^2/g)\hat{b},\quad c=(\sigma^2/g)\hat{c},\quad t=\sigma\hat{t}, \tag{3.1}$$

with corresponding definitions for ζ, $x^{(1)}$, $x^{(2)}$, $y^{(1)}$, etc..

From (2.5) and (2.6) we obtain, assuming that ν is a function of $\hat{c}$ alone,

$$x_{tt}^{(1)}=-p_a^{(1)}-z_a^{(1)}+\tfrac{1}{2}d_c[z_{ta}^{(1)}+x_{tc}^{(1)}]+\tfrac{1}{2}d_0[x_{taa}^{(1)}+x_{tcc}^{(1)}],$$

$$z_{tt}^{(1)}=-p_c^{(1)}-z_c^{(1)}+d_c z_{tc}^{(1)}+\tfrac{1}{2}d_0[z_{taa}^{(1)}+z_{tcc}^{(1)}],$$

$$x_a^{(1)}+z_c^{(1)}=0, \tag{3.2}$$

with $d_0(c)=2\nu\sigma^3/g^2$ and $d_c(c)=2\nu_{\hat{c}}\sigma/g$.

b. Solution

Following Lamb (1932, Art. 349), we define functions ϕ and ψ, such that

$$x_t^{(1)}=-\phi_a-\psi_c$$
$$z_t^{(1)}=-\phi_c+\psi_a. \tag{3.3}$$

We obtain

$$\nabla_L{}^2\phi=0 \tag{3.4}$$

$$-\tfrac{1}{2}d_0\nabla_L{}^4\psi+\nabla_L{}^2\psi_t+d_c\nabla_L{}^2\psi_c+\tfrac{1}{2}d_{cc}(\psi_{aa}-\psi_{cc})=d_{cc}\phi_{ac}, \tag{3.5}$$

where

$$\nabla_L{}^2\equiv\partial^2/\partial a^2+\partial^2/\partial c^2 \quad\text{and}\quad d_{cc}=2\nu_{\hat{c}\hat{c}}/\sigma.$$

We now assume that we have (almost) monochromatic traveling wave solutions to (3.4) and (3.5), of the form

$$\phi=\Phi(c)E(a)N(t),$$
$$\psi=\Psi(c)E(a)N(t), \tag{3.6}$$

where

$$E(a)=\exp(i\kappa a)\exp(-\kappa d_s a)$$
$$N(t)=\exp(-it)\exp(-d_t t).$$

The parameter κ is a positive nondimensional wavenumber [assumed to be O(1)] and the parameters d_s and d_t are real decay coefficients. The parameters d_s and d_t can be either positive or negative, but their moduli must be much less than 1.

From (3.4) and (3.6) we obtain

$$\Phi=AK(c), \tag{3.7}$$

where $K(c)=\exp[\kappa(1+id_s)c]$ (the solution is assumed to decay to zero as $c\to-\infty$) and A is an arbitrary amplitude. Substituting (3.6) and (3.7) into (3.5), we obtain the following equation for Ψ, where we have assumed that d_0, d_c and d_{cc} are all small and have ignored them in comparison with terms of order 1:

$$-\tfrac{1}{2}d_0\Psi_{cccc}+d_c\Psi_{ccc}+i\Psi_{cc}-\kappa^2 d_c\Psi_c+i\kappa^2\Psi=iAd_{cc}\kappa^2K(c). \tag{3.8}$$

(Note that in the rest of this paper, small terms will often be ignored without it being specifically stated).

We use boundary layer theory to find an approximate solution to (3.8) (e.g., see Bender and Orszag, 1978, Chap. 9). The domain of the solution to the equation consists of:

(i) an *outer region* where the solution (Ψ^o) varies relatively slowly and we can ignore the terms with small coefficients on the left-hand side,

(ii) an *inner region* (boundary layer), near $c=0$, where the solution (Ψ^i) varies rapidly.

In the outer region, (3.8) becomes

$$\Psi_{cc}^o-\kappa^2\Psi^o=-Ad_{cc}\kappa^2K(c). \tag{3.9}$$

This is a linear inhomogeneous second order ordinary differential equation, whose solution we define as $\chi(c)A$; we assume that $\chi(0)=O(d)$, where d is a typical value of the greatest of the parameters $|d_s|$, $|d_t|$, d_0 within the depth of wave influence [$-c=O(1)$].

In the particular case where we have a constant value of d_0 (constant eddy viscosity) from the surface down to a depth $-c'$ with a subsequent linear variation of d_0 (see Fig. 2):

$$d_0=D_0,\quad c'\leqslant c\leqslant 0,$$
$$d_0=D_0+D_c(c'-c),\quad c\leqslant c', \tag{3.10}$$

the right-hand side of (3.9) will have a delta-function behavior (here we relax in an appropriate manner the criterion that $|d_{cc}|\ll 1$). We then have

$$\chi(c)=\tfrac{1}{2}\kappa D_c e^{\kappa c'}e^{-\kappa|c-c'|}+He^c, \tag{3.11}$$

where H is an arbitrary constant, with $H=O(d)$ under the condition $\chi(0)=O(d)$. For a more general behavior of d_{cc}, we obtain $\chi(c)$ by performing an appropriate weighted integration with respect to c' of solutions of the form (3.11).

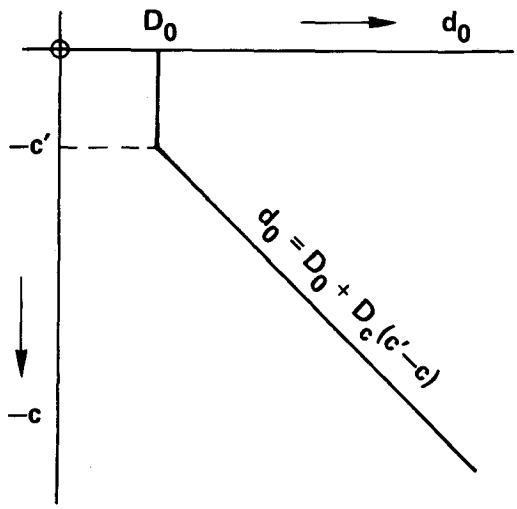

FIG. 2. The piecewise linear profile of d_0 described in (3.10).

To determine the solution of (3.8) in the inner region, we define a "stretched" vertical coordinate $C = \gamma c$. The dimensionless length scale $(1/\gamma)$ can be thought of as the "thickness" of the boundary layer. Equation (3.8) then becomes, in the inner region

$$-\frac{1}{2}d_0\gamma^4\Psi^i_{CCCC} - i\gamma^2\Psi^i_{CC} + i\kappa^2\Psi = 0, \quad (3.12)$$

where we have assumed $d_c = 0$ within the inner region. If we have $\gamma = [d_0(0)]^{-1/2}$, (3.12) becomes

$$\Psi^i_{CCCC} + 2i\Psi^i_{CC} = 0, \quad (3.13)$$

where we ignore the third term on the left-hand side of (3.12) in comparison with the others. The boundary layer thickness $(1/\gamma)$ is then equal to $[d_0(0)]^{1/2} \ll 1$, and we have a solution

$$\Psi^i = BM(c), \quad (3.14)$$

where $M(c) = \exp[d_0^{-1/2}(1 - i)c]$ and B is a constant. (Note that we again assume that the solution tends to zero as $c \to -\infty$).

We can obtain an approximation to Ψ which is valid in both the outer and inner regions by simply adding together Ψ^o and Ψ^i,

$$\Psi = A\chi(c) + BM(c), \quad (3.15)$$

since $\Psi^i \to 0$ rapidly for $c < -1/\gamma$ and Ψ^o varies so slowly that it would give rise to a negligible contribution if it were added to Ψ^i in (3.13).

From (3.3), (3.6), (3.7) and (3.15), we obtain, retaining the lowest-order terms (in d) proportional to $M(c)$, $\chi(c)$ and $\chi_c(c)$, and the lowest and next-lowest order terms proportional to $K(c)$:

$$x^{(1)} = [\kappa(1 + id_s + id_t)AK(c) - i\kappa(1 - i)d_0^{-1/2}BM(c) - iA\chi_c(c)]E(a)N(t),$$

$$z^{(1)} = [-i\kappa(1 + id_s + id_t)AK(c) - \kappa BM(c) - \kappa A\chi(c)]E(a)N(t). \quad (3.16)$$

Substituting (3.16) into (3.2) and retaining terms up to $O(1)\cdot BM(c)$, $O(1)\cdot A\chi(c)$ and $O(d)\cdot AK(c)$, we obtain the following expression for the dynamic pressure:

$$p^{(1)} = \{[-i(1 - id_t) + i\kappa(1 + id_s + id_t) - \kappa d_c]AK(c) + [-(1 - i)d_0^{-1/2} + \kappa^2(1 - i)d_0^{-1/2} + \kappa + \kappa d_0^{-1}d_c]BM(c) + [-\kappa^{-1}\chi_c(c) + \kappa\chi(c)]A\}E(a)N(t). \quad (3.17)$$

c. Boundary conditions

Chang (1969) and Weber (1983a,b) determined the following boundary conditions at the free surface ($c = 0$), to $O(\epsilon^2)$:

$$P^{(zz)} = -p_0 + \epsilon[-p^{(1)} + d_0 z^{(1)}_{tc}] + \epsilon^2\left\{-p^{(2)} + \frac{1}{2}d_0[2z^{(2)}_{tc} + 2x^{(1)}_a z^{(1)}_{tc} - 2x^{(1)}_c z^{(1)}_{ta} - x^{(1)}_{tc} z^{(1)}_a - z^{(1)}_{ta} z^{(1)}_a]\right\}, \quad (3.18)$$

$$P^{(xz)} = \frac{1}{2}\epsilon d_0[x^{(1)}_{tc} + z^{(1)}_{ta}] + \epsilon^2\left\{p^{(1)}z^{(1)}_a + \frac{1}{2}d_0[x^{(2)}_{tc} + z^{(2)}_{ta} + x^{(1)}_a x^{(1)}_{tc} - x^{(1)}_{ta}x^{(1)}_c + z^{(1)}_{ta}z^{(1)}_c - z^{(1)}_a z^{(1)}_{tc} - 2x^{(1)}_{ta}z^{(1)}_a]\right\}, \quad (3.19)$$

where $P^{(zz)}$ and $P^{(xz)}$ are the nondimensional vertical and horizontal external stresses respectively and $p_0 = (\sigma^2/\rho g^2)\hat{p}_0$ is the nondimensional atmospheric pressure. We expand the external stresses as follows, in powers of ϵ:

$$P^{(zz)} = -p_0 + \epsilon(\Delta_{zr} + i\Delta_{zi})E(a)N(t) + O(\epsilon^2), \quad (3.20)$$

$$P^{(xz)} = \epsilon(\Delta_{xr} + i\Delta_{xi})E(a)N(t) + \epsilon^2 P^{(xz)(2)} + O(\epsilon^3). \quad (3.21)$$

In formulating (3.20) and (3.21) we assume that the $O(\epsilon)$ surface stress is oscillatory, with the same frequency and wavenumber as the $O(\epsilon)$ surface wave field, and we will show that this stress component contributes to wave growth (Lamb, 1932, Art. 349; Miles, 1957). We include all other contributions to the surface stress in the $O(\epsilon^2)$ and higher-order terms, apart from the constant atmospheric pressure. The real quantities Δ_{zr} and Δ_{zi} are the components of the vertical stress variation in quadrature and in antiphase with the surface elevation, respectively, and the quantities Δ_{xr} and Δ_{xi} (each also real) are the corresponding components of the horizontal stress variation. We now write:

$$\kappa = 1 + \delta, \quad (3.22)$$

$$B = B_r + iB_i, \quad (3.23)$$

where δ is real (the imaginary part of the wavenumber is equal to κd_s), as are B_r and B_i. From (3.19),

$$B_i = -\Delta_{xr}, \quad (3.24)$$

$$B_r = Ad_0(0) + \Delta_{xi}. \quad (3.25)$$

Normalizing the solutions (3.16) and (3.17) with $A = 1$, we find that $\epsilon = \zeta_0$, the nondimensional wave amplitude near $a = t = 0$. The small parameter ϵ is thus approximately equal to the *physical* amplitude of the surface slope near $\hat{a} = \hat{t} = 0$, provided that $|B| \ll A$. With this assumption, the perturbation expansion should be valid near a particular location and time if the *wave slope* $\equiv \max[|\partial\hat{z}/\partial\hat{a}|_{(c=0)}] \approx \epsilon|E(a)N(t)| \ll 1$.

If we now use the boundary condition (3.19), we obtain

$$\delta = \Delta_{xr} - \Delta_{zi}, \tag{3.26}$$

$$d_t + \tfrac{1}{2}d_s = d_0(0) + \tfrac{1}{2}[\chi(0) - \chi_c(0)] + \tfrac{1}{2}\Delta_{zr} + \tfrac{1}{2}\Delta_{xi}. \tag{3.27}$$

Equation (3.26) provides a correction to the deep-water wave dispersion relation ($\kappa = 1$). It will be a small correction (which we assume) if Δ_{xr} and Δ_{zi} are small, and we can extend the definition of d so that they are both O(d). We find, in fact, that δ plays very little part in the subsequent analysis and we can usually assume $\kappa = 1$, e.g. in (3.28) below. The left-hand side of (3.27) gives the rate of wave decay in a frame moving with the group velocity. In the absence of surface stress variations, i.e., if all the Δ-parameters are zero, the decay of the waves is given by

$$\left[d_0 + \tfrac{1}{2}(\chi - \chi_c)\right]_{c=0} = d_0(0) + \tfrac{1}{2}\int_{-\infty}^{0} d_{cc}(c')e^{2c'}dc'. \tag{3.28}$$

The last two terms in (3.27) represent the tendency for wave growth as a result of cyclic vertical and horizontal surface stress variations, respectively. Note that for wave *growth* to take place, the sum of the two terms must be negative, and they should also be O(d) since all the other terms are O(d). Consequently, by (3.24) and (3.25), B = O(d).

4. Second-order equations

a. Derivation

The O(ϵ^2) parts of (2.5), when averaged over one (monochromatic) wave cycle and expressed in terms of non-dimensional coordinates and variables, are

$$\overline{x_{tt}^{(2)}} - (f/\sigma)\overline{y_t^{(2)}} + \overline{z_a^{(2)}} + \overline{p_a^{(2)}} - \tfrac{1}{2}d_0[\overline{x_{taa}^{(2)}} + \overline{x_{tcc}^{(2)}}] - \tfrac{1}{2}d_c[\overline{x_{tc}^{(2)}} + \overline{z_{ta}^{(2)}}] = \overline{p_a^{(1)}x_a^{(1)}} + \overline{p_c^{(1)}z_a^{(1)}} + \tfrac{1}{2}d_c[-2\overline{x_{ta}^{(1)}z_a^{(1)}} + \overline{z_{ta}^{(1)}x_a^{(1)}}$$
$$+ \overline{z_{ta}^{(1)}z_c^{(1)}} - \overline{z_{tc}^{(1)}z_a^{(1)}} + 2\overline{x_{tc}^{(1)}x_a^{(1)}} - \overline{x_{ta}^{(1)}x_c^{(1)}}] + \tfrac{1}{2}d_0[-2\overline{x_a^{(1)}x_{taa}^{(1)}} - 2\overline{z_c^{(1)}x_{tcc}^{(1)}} - 2\overline{z_a^{(1)}x_{tac}^{(1)}} - 2\overline{x_c^{(1)}x_{tac}^{(1)}}$$
$$- \overline{x_{ta}^{(1)}x_{aa}^{(1)}} - \overline{x_{ta}^{(1)}x_{cc}^{(1)}} - \overline{x_{tc}^{(1)}z_{aa}^{(1)}} - \overline{x_{tc}^{(1)}z_{cc}^{(1)}}], \tag{4.1}$$

$$\overline{y_{tt}^{(2)}} + (f/\sigma)\overline{x_t^{(2)}} - \tfrac{1}{2}d_0\overline{y_{tcc}^{(2)}} - \tfrac{1}{2}d_c\overline{y_{tc}^{(2)}} = 0, \tag{4.2}$$

$$\overline{z_{tt}^{(2)}} + \overline{z_c^{(2)}} + \overline{p_c^{(2)}} - \tfrac{1}{2}d_0[\overline{z_{taa}^{(2)}} + \overline{z_{tcc}^{(2)}}] - d_c\overline{z_{tc}^{(2)}} = \overline{p_a^{(1)}x_c^{(1)}} + \overline{p_c^{(1)}z_c^{(1)}} + \overline{z_a^{(1)}x_c^{(1)}} + \overline{z_c^{(1)}z_c^{(1)}} + \tfrac{1}{2}d_c[-\overline{x_{tc}^{(1)}z_a^{(1)}} - \overline{z_{ta}^{(1)}z_a^{(1)}}$$
$$+ 4\overline{z_{tc}^{(1)}x_a^{(1)}} - 2\overline{z_{ta}^{(1)}x_c^{(1)}}] + \tfrac{1}{2}d_0[-2\overline{x_a^{(1)}z_{taa}^{(1)}} - 2\overline{z_c^{(1)}z_{tcc}^{(1)}} - 2\overline{z_a^{(1)}z_{tac}^{(1)}} - 2\overline{x_c^{(1)}z_{tac}^{(1)}} - \overline{z_{ta}^{(1)}x_{aa}^{(1)}} - \overline{z_{ta}^{(1)}x_{cc}^{(1)}} - \overline{z_{tc}^{(1)}z_{aa}^{(1)}} - \overline{z_{tc}^{(1)}z_{cc}^{(1)}}], \tag{4.3}$$

where the overbars denote the averages. Note that there are some discrepancies between the above equations and Pierson's (1962) expansion, which is the result of the presence of several errors in Pierson's equations.

Differentiating (4.1) with respect to c and (4.3) with respect to a, subtracting and reintegrating, we obtain, using complex notation with $W \equiv \epsilon^2[\overline{x_t^{(2)}} + i\overline{y_t^{(2)}}]$:

$$W_t + i(f/\sigma)W - (\partial/\partial c)\left(\tfrac{1}{2}d_0W_c\right)$$
$$= 2\zeta_a{}^2\{-e^{2c}(d_t + d_0 + d_c) + d_0{}^{-1/2}e^{\gamma c}[(d_0 + \Delta_{xi})$$
$$\times(\cos\gamma c - \sin\gamma c) - \Delta_{xr}(\cos\gamma c + \sin\gamma c)]\}, \tag{4.4}$$

where $\zeta_a = \zeta_0 \exp(-d_s a - d_t t)$ is the wave amplitude.

b. Boundary condition

From the O(ϵ^2) part of (3.19) we obtain

$$\tfrac{1}{2}d_0W_c = \epsilon^2\overline{P^{(xz)(2)}} - \zeta_a{}^2[d_0 + \tfrac{3}{2}\Delta_{xi}$$
$$+ \tfrac{1}{2}(\chi - \chi_c) - d_t - \tfrac{1}{2}d_s], \quad c = 0. \tag{4.5}$$

c. Splitting of the solution

As in J1, we split W into three parts: a vorticity layer solution $w^{(v)}$, a Stokes drift $w^{(s)}$ and a quasi-Eulerian current $W^{(r)}$:

$$W = W^{(r)} + w^{(s)} + w^{(v)}. \tag{4.6}$$

We then have:

$$w^{(v)} = -2d_0{}^{-1/2}\zeta_a{}^2e^{\gamma c}[(d_0 + \Delta_{xi})(\cos\gamma c + \sin\gamma c)$$
$$+ \Delta_{xr}(\cos\gamma c - \sin\gamma c)], \tag{4.7}$$

$$w^{(s)} = \zeta_a{}^2e^{2c}, \tag{4.8}$$

with $W^{(r)}$ satisfying the following differential equation:

$$W_t^{(r)} + i(f/\sigma)W^{(r)} - (\partial/\partial c)\left[\frac{1}{2}d_0 W_c^{(r)}\right] = [-d_c - i(f/\sigma)]w^{(s)}, \quad (4.9)$$

and boundary condition:

$$\frac{1}{2}d_0 W^{(r)} = \epsilon^2\overline{P^{(xz)(2)}} + w^{(s)}\left[d_t + \frac{1}{2}d_s - \frac{1}{2}(\chi - \chi_c) + \frac{1}{2}\Delta_{xi}\right], \quad c = 0. \quad (4.10)$$

d. Momentum balance

The $O(\epsilon)$ oscillatory part of the horizontal surface stress, $\epsilon P^{(xz)(1)} = \epsilon(\Delta_{xr} + i\Delta_{xi})E(a)N(t)$, contributes a net mean momentum flux. We see this by averaging it over one wavelength, ignoring small terms where appropriate and noting that $dc = 0$ since we are integrating along the sea surface:

$$\begin{aligned}\frac{\kappa}{2\pi}\int_0^{2\pi/\kappa} \epsilon P^{(xz)(1)}dx &= \frac{\kappa}{2\pi}\int_{a=0}^{a=2\pi/\kappa} \epsilon P^{(xz)(1)}\left(\frac{\partial x}{\partial a}da + \frac{\partial x}{\partial c}dc\right)\\ &= \epsilon\overline{P^{(xz)(1)}[1 + \epsilon x_a^{(1)}]}\\ &= \frac{1}{2}\epsilon^2\Delta_{xi}|E(a)N(t)|^2\\ &= \frac{1}{2}\zeta_a{}^2\Delta_{xi}. \end{aligned} \quad (4.11)$$

This momentum flux contribution explains why Weber (1983b) obtained an unbounded steady state mass transport velocity for infinite depth in the absence of the Earth's rotation for the case where the waves were maintained at constant amplitude by an oscillatory horizontal surface stress, even when what he defined as the "mean horizontal wind stress" was zero. Weber defined the mean horizontal wind stress as the mean $O(\epsilon^2)$ part of (3.21), whereas it would be more sensible to define it so that it provides the *total* momentum flux through the sea surface. We thus define the dimensionless wind stress $\tau = (\sigma^2/\rho g^2)\hat{\tau}$ as the sum of the mean contributions from the $O(\epsilon)$ and $O(\epsilon^2)$ parts of $P^{(xz)}$. Equation (4.10) then becomes:

$$\begin{aligned}\frac{1}{2}d_0 W_c^{(r)} &= \tau + w^{(s)}\left[d_t + \frac{1}{2}d_s - \frac{1}{2}(\chi - \chi_c)\right]\\ &= \tau + \zeta_a{}^2\left[d_t + \frac{1}{2}d_s - \frac{1}{2}(\chi - \chi_c)\right], \quad c = 0. \end{aligned} \quad (4.12)$$

With this definition of τ, the behavior of $W^{(r)}$ is independent of the partition of the rate of energy input to the waves between the horizontal and vertical components of the oscillatory $O(\epsilon)$ surface stress.

Equations (4.9) and (4.12) reduce to the corresponding equations in J1 if d_0 is independent of c; i.e., if the eddy viscosity is constant. In the case of constant eddy viscosity, momentum which disappears from the wave field due to wave dissipation is transferred to the quasi-Eulerian current at the surface by means of the $\zeta_a{}^2(d_t + \frac{1}{2}d_s)$ part of (4.12), and thereafter diffuses into the water column. This effect is in agreement with Longuet-Higgins' (1970) observation that the local stress exerted by the waves is directly proportional to the local rate of dissipation of wave energy.

In the case of depth-varying viscosity, the momentum transfer at the surface is reduced by an amount $\frac{1}{2}\zeta_a{}^2[\chi - \chi_c]_{c=0}$, which is balanced by the $-d_c w^{(s)}$ source term in (4.9). The equivalence of the two contributions can be demonstrated by integrating (3.28) by parts, noting that $d_c = 0$ at the surface.

5. Solutions

a. Introduction

Equations (4.9) and (4.12) become, in terms of dimensional quantities,

$$\hat{W}_{\hat{t}}^{(r)} + if\hat{W}^{(r)} - (\partial/\partial\hat{c})[\nu\hat{W}_{\hat{c}}^{(r)}] = (-2\nu_{\hat{c}}\hat{\kappa} - if)\hat{w}^{(s)}, \quad (5.1)$$

$$\nu\hat{W}_{\hat{c}}^{(r)} = \hat{\tau}/\rho + \hat{w}^{(s)}(\sigma/\hat{\kappa})\left[d_t + \frac{1}{2}d_s - \frac{1}{2}(\chi - \chi_c)\right], \quad \hat{c} = 0, \quad (5.2)$$

where $\hat{W}^{(r)} = (g/\sigma)W^{(r)}$, $\hat{w}^{(s)} = (g/\sigma)w^{(s)}$ and $\hat{\kappa} = (\sigma^2/g)\kappa$.

Equations (5.1) and (5.2) were solved numerically with a variable vertical grid spacing, which was smallest near the sea surface. The system was started from rest at $\hat{t} = 0$, by applying a wind stress in the x-direction together with a monochromatic wave field with wavenumber vector in the same direction. The wave field was assumed to be locally uniform in space and time ($d_s = d_t = 0$), dissipation of the waves by the eddy viscosity being balanced by energy input from the cyclic stress variations of (3.20) and (3.21). To preserve self-consistency, we represent all dissipative processes, including wave breaking, by a suitable eddy viscosity profile.

The wind stress $\hat{\tau}$ and friction velocity u_* were assumed to be given by

$$\hat{\tau}/\rho = u_*^2 = c_{10}(\rho_a/\rho)U_{10}{}^2, \quad (5.3)$$

where U_{10} is the wind speed at the 10 m level and c_{10} is the drag coefficient. We used the relations between U_{10}, c_{10}, wavelength and wave amplitude which were used by Weber (1983b). Table 1 shows the values of the relevant parameters. The wave slope ($=\zeta_a$) is equal to 0.17 throughout, which is perhaps rather large for the perturbation expansion to be strictly valid, particularly since we assume that wave breaking (an obviously strongly nonlinear wave phenomenon) is the physical reason for the waves keeping a constant amplitude in the presence of the cyclic surface stress variations. [Note that what is commonly called the wave

TABLE 1. Parameter values for numerical simulation runs.

Coriolis parameter: $f = 1.26 \times 10^{-4}\ s^{-1}$
Von Kármán's constant: $\kappa_K = 0.4$
Water:air density ratio: $\rho/\rho_a = 800$
Acceleration due to gravity: $g = 9.8\ m\ s^{-2}$
Water depth: 300 m (150 m for simulation 4)

Run	Wind speed ($m\ s^{-1}$)	Drag coefficient c_{10}	Wave: Amplitude $\hat{\zeta}_0$ (m)	Wave: Period (s)	Eddy viscosity ($m^2\ s^{-1}$): From surface to depth $-\hat{c}_0$	Eddy viscosity ($m^2\ s^{-1}$): At depth $-\hat{c}_1$	Eddy viscosity ($m^2\ s^{-1}$): Gradient below depth $-\hat{c}_1$ ($m\ s^{-1}$)	Depths of eddy viscosity "kinks": $-\hat{c}_0$ (m)	Depths of eddy viscosity "kinks": $-\hat{c}_1$ (m)
1	10	1.8×10^{-3}	0.88	4.5	1.54×10^{-2}	3.07×10^{-2}	6.0×10^{-3}	2.56	5.1
2	10	1.8×10^{-3}	0.88	4.5	3.07×10^{-2}	3.07×10^{-2}	6.0×10^{-3}	2.56	5.1
3	10	1.8×10^{-3}	0.88	4.5	4.61×10^{-2}	3.07×10^{-2}	6.0×10^{-3}	2.56	5.1
4	5	1.8×10^{-3}	0.221	2.27	3.8×10^{-3}	3.8×10^{-3}	3.0×10^{-3}	0.64	1.28
5	15	1.8×10^{-3}	1.99	6.8	0.104	0.104	9.0×10^{-3}	5.8	11.5
6	20	2.7×10^{-3}	3.6	9.2	0.310	0.310	1.47×10^{-2}	10.6	21.1
7	25	2.7×10^{-3}	5.7	11.5	0.61	0.61	1.84×10^{-2}	16.5	33.0
8	30	2.7×10^{-3}	8.2	13.8	1.05	1.05	2.21×10^{-2}	23.7	47

steepness = wave height/wavelength, is equal to $\zeta_a/\pi \approx 0.055$.]

b. *Vertical profile of eddy viscosity*

Except for within a layer near the surface, the eddy viscosity was assumed to be proportional to depth, as in Madsen (1977):

$$\nu = -\kappa_K u_* \hat{c}, \tag{5.4}$$

where κ_K is von Kármán's constant. Thorpe (1984), from acoustic observations of bubbles generated by breaking waves, concluded that the eddy viscosity profile within the upper mixed layer was indeed probably of the form (5.4), apart from in the zone directly affected by breaking waves. He estimated this zone to have a thickness of the order of 10 times the wave amplitude $\hat{\zeta}_a = (g/\sigma^2)\zeta_a$. Breaking waves will obviously have a considerable effect for the steady state wind and wave forcing considered in the numerical simulations presented here, and can thus be expected to increase the eddy viscosity significantly above the values given by (5.4).

We have chosen three types of profile, referred to as the "low", "medium" and "high" surface eddy viscosity profiles, which are shown in Fig. 3. The "medium" profile has a constant eddy viscosity from the surface down to a depth of $1/\hat{\kappa}$ (roughly $6\hat{\zeta}_a$), the "low" profile has a constant eddy viscosity from the surface down to a depth of $1/(2\hat{\kappa})$ (the Stokes depth), and the "high" profile has a constant eddy viscosity equal to 1.5 times that of the "medium" profile from the surface down to a depth of $1/(2\hat{\kappa})$, with a subsequent linear decrease down to the depth of $1/\hat{\kappa}$. Using such piecewise-linear eddy viscosity profiles, it is simple to calculate the appropriate surface values of $\chi - \chi_c$ for the surface boundary condition, using a modified form of (3.11) to take account of the presence of two discontinuities in d_c.

The water depth was set equal to 300 m, which is sufficiently deep for the deep-water wave dispersion relation to apply, apart from simulation 4 (wind speed 5 $m\ s^{-1}$), where the water depth was set to 150 m in order to keep the computer time within reasonable bounds, given the finer vertical resolution required for the small wavelength. A slip condition [$\hat{W}^{(r)}_{\hat{c}} = 0$] was applied at the bottom boundary.

c. *Results*

Figures 4, 5 and 6 show the development in time of the Lagrangian mean current, $\hat{W}^{(r)} + \hat{w}^{(s)}$, the vorticity layer current being neglected since it is $O[d_0^{1/2}\hat{w}^{(s)}]$, from the surface down to 20 m depth, for a wind speed of 10 $m\ s^{-1}$ and "low", "medium" and "high" surface eddy viscosity respectively (simulations 1, 2 and 3). The current was plotted every ¼ pendulum hour, the pronounced kinks in the "low" eddy viscosity curves being at $\hat{t} = ¼$ pendulum hour. The points on the curves correspond to $\hat{t} = 0^+, 1, 2, \cdots, 15$ pendulum hours. The development of the quasi-Eulerian current can be obtained by displacing each of the curves so that the $\hat{t} = 0^+$ value is moved to the origin.

The "high" and "medium" eddy viscosity profiles appear to give results which are roughly in accord with observations, but the "low" eddy viscosity profile shows anomalies near the surface; at the surface, the quasi-Eulerian current is initially in the opposite direction to the wind. This is a result of the wind stress feeding insufficient momentum into the wave field to balance the part of the wave dissipation due to the eddy viscosity being different from its surface value: the first term on

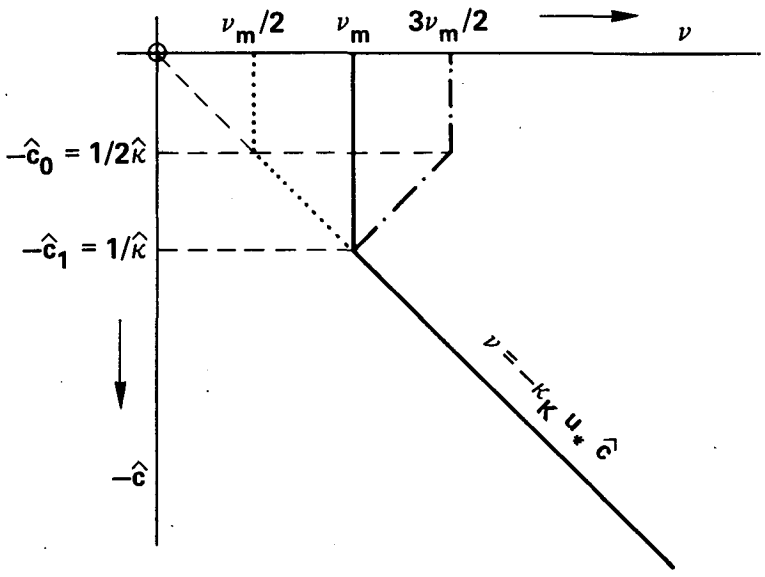

FIG. 3. The piecewise linear eddy viscosity profiles used in the simulations. Dotted line: "low" profile. Solid line: "medium" profile. Dash-dotted line: "high" profile. (ν_m = "medium" value of surface eddy viscosity.)

the right-hand side of (5.2) is smaller in magnitude than the second term. This condition is unlikely to be realized in practice, it being more reasonable to believe that the vertical shear in the quasi-Eulerian current near the surface is in the same direction as the wind stress. It is possible that the wind drag coefficient should be higher than we have assumed (see Donelan, 1982), but for the purposes of this paper we did not alter the drag coefficient, and assumed that we have a "medium" eddy viscosity profile when performing the simulations for different wind speeds.

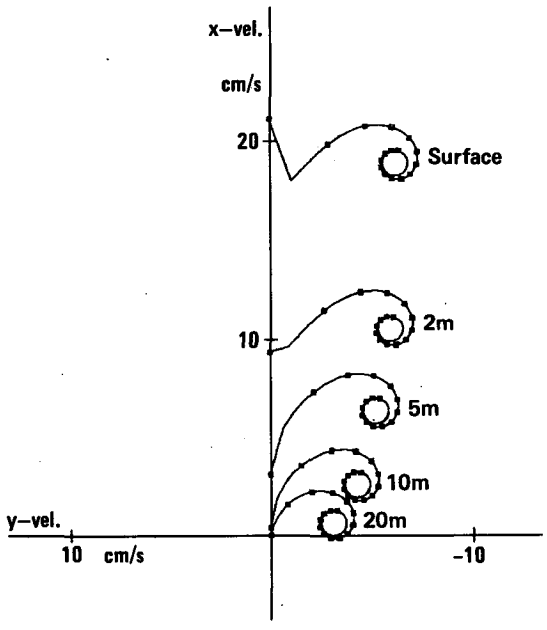

FIG. 4. Development in time (0 to 48 pendulum hours) of the Lagrangian current for a wind speed of 10 m s^{-1} ($\hat{t} > 0$). Simulation 1—see Table 1 for details ("low" surface eddy viscosity). The dots mark each pendulum hour from 0 to 15.

Madsen's (1977) results are also plotted in Fig. 5, where his nondimensional current ($=\kappa_K \hat{W}/u_*$) is converted to the appropriate physical values. The two models give results which are surprisingly close, even though Madsen does not take account of surface waves. The agreement is best at greater depths, where the wave influence is small and where the eddy viscosities are the same in both models. Madsen's surface current values are somewhat uncertain, since his solution has a singularity at $\hat{z} = 0$ (where $\nu = 0$), and he had to choose a small negative value for $\hat{z}$ to represent the physical surface. Madsen's time development of the surface current appears to have a very similar form to the present model results, particularly for the "high" eddy viscosity case (Fig. 6), even though Madsen's current actually increases continuously from zero instead of increasing discontinuously from zero to the Stokes drift at $t = 0^+$.

Figure 7 shows the evolution of the quasi-Eulerian current from the surface down to 100 m depth, for a 10 m s^{-1} wind and the "medium" eddy viscosity profile. For depths of 20 m and greater, the Lagrangian mean current will be almost identical to the quasi-Eulerian current. Madsen's steady state results are also shown: they are in good agreement for greater depths, but diverge greatly from the present results closer to the surface. Figures 8 and 9 show the evolution of the La-

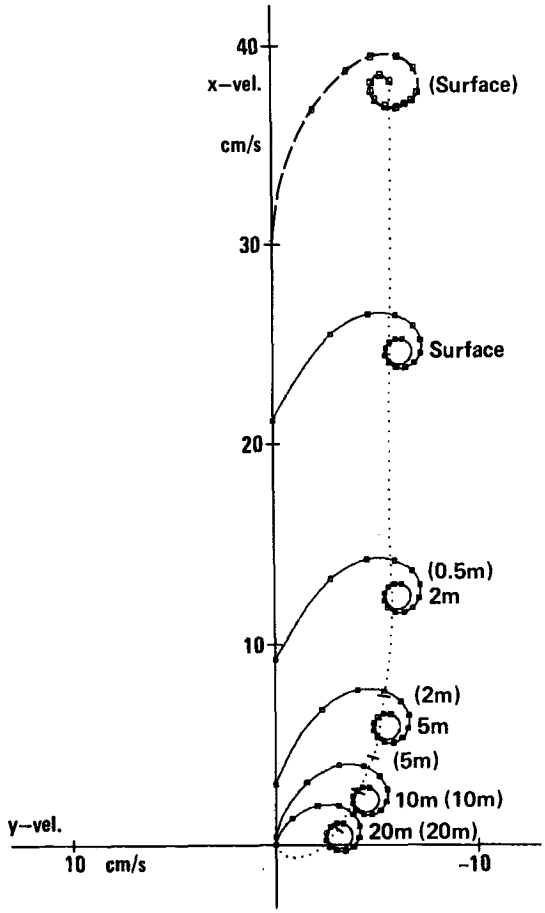

FIG. 5. As in Fig. 4 but for simulation 2 (wind speed 10 m s^{-1}, "medium" surface eddy viscosity). Madsen's (1977) results are also shown, with text in parentheses. Dotted line: Madsen's steady-state current profile; broken line: Madsen's time development of surface current.

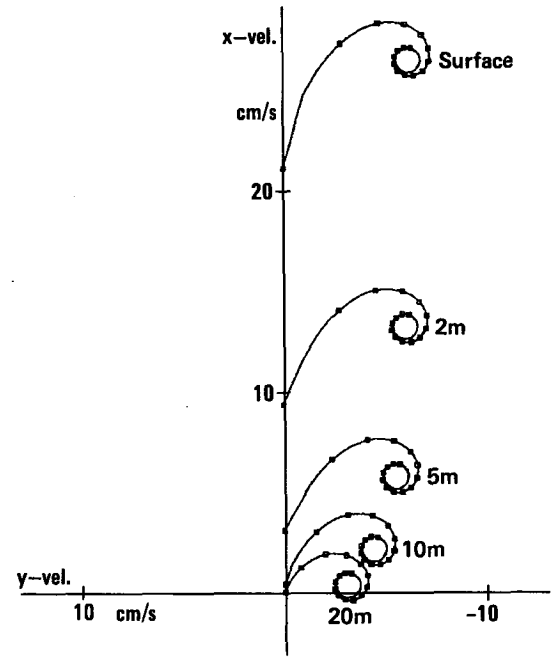

FIG. 6. As in Fig. 4 but for simulation 3 (wind speed 10 m s^{-1}, "high" surface eddy viscosity).

grangian and quasi-Eulerian current respectively for wind speeds of 10 and 25 m s^{-1}. The relatively slower decrease of the current with depth for the 25 m s^{-1} wind, as a result of the greater depth of wave influence and greater values of eddy viscosity, is clearly seen. The large circular oscillations of the 25 m s^{-1} current are inertial oscillations which persist after the influence of the wind and waves has penetrated through the whole depth; the slip boundary condition means that the oscillations are unable to dissipate. Smaller oscillations are evident in the 10 m s^{-1} current.

Figure 10 shows a plot of the long-term average Lagrangian and quasi-Eulerian surface current as a fraction of the wind speed, and its direction (to the right of the wind and wave direction), for "medium" eddy viscosity profiles with winds of between 5 and 30 m s^{-1}. The long-term average was calculated by finding the centers of the inertial-oscillation circles (see Figs. 4–9). The Lagrangian currents obtained are a roughly constant fraction of wind speed (between 2.2% and 2.8%), and are in reasonably good agreement with drift observations. The drift direction is closer to the wind direction (between 12° and 17° to the right) than in the constant eddy viscosity case (between 20° and 30° to the right according to Weber, 1983b), which is an improvement when compared with drift observations. The quasi-Eulerian currents are much smaller and are turned much more to the right than the Lagrangian

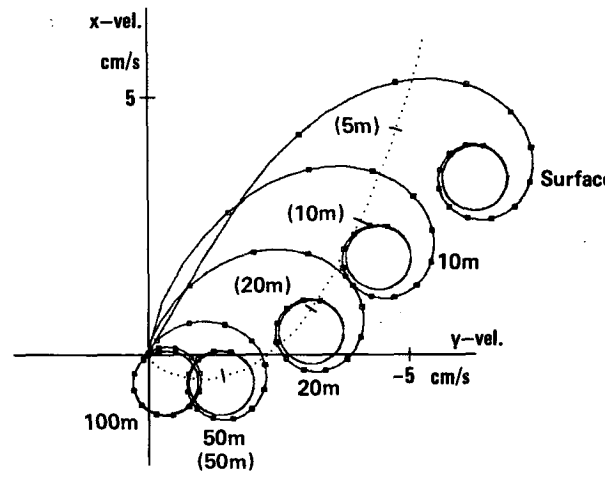

FIG. 7. Development in time of the quasi-Eulerian current for simulation 2 (wind speed 10 m s^{-1}, "medium" surface eddy viscosity). The dotted line and text in parentheses show Madsen's (1977) steady-state current profile.

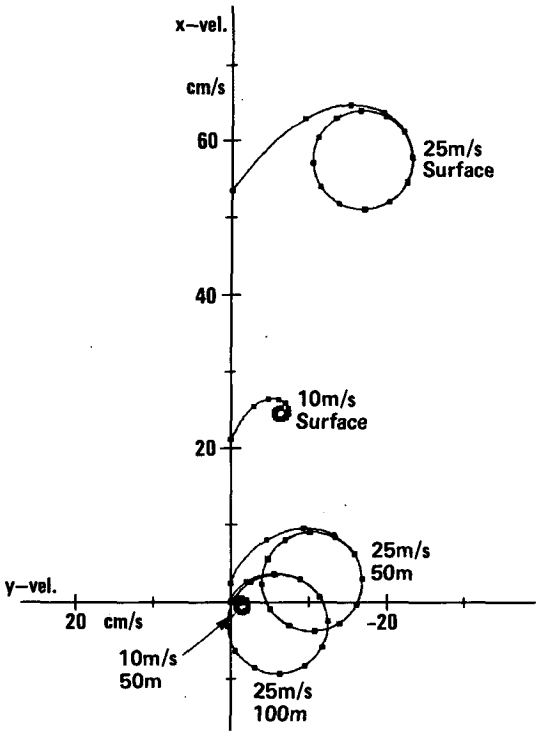

FIG. 8. Development in time of the Lagrangian current for simulations 2 (wind speed 10 m s^{-1}) and 7 (wind speed 25 m s^{-1}).

currents. It is, however, difficult to compare them with observations, since current meters moored near the surface, even if they perform perfect vector averaging, are liable to produce results which differ from the Eulerian mean current by an amount of the same order of magnitude as the Stokes drift at the surface, as a result of mooring motion (Pollard, 1973).

The present model gives results which are in agreement with those of Madsen (1977) below the zone of wave influence. Within the wave zone, agreement with Madsen's results is better for the Lagrangian mean rather than the Eulerian mean current. This is probably because the Lagrangian mean current can be regarded as a "truer" current in the dynamical sense: it represents directly the movement of particles, and is the current which should be used when calculating the Coriolis force [compare (4.4) and (4.9)].

6. Applications

a. Introduction

The theory developed in this paper can be used to calculate the current induced by an observed wind and directional wave field, if we are able to extend it to cover a general directional wave spectrum, if we can estimate the spatial variation in the wave field (d_s), and if it is possible to make an estimate of the effective eddy viscosity profile.

b. General directional wave spectrum

For a random wave field, composed of many different sinusoidal components with uncorrelated phases, the time-averaged products of pairs of linear functions of the $O(\epsilon)$ velocity components, pressure, etc. will be zero unless each factor in the product refers to the same wavenumber vector. (We assume that we do not have standing waves, so that wave components coming from

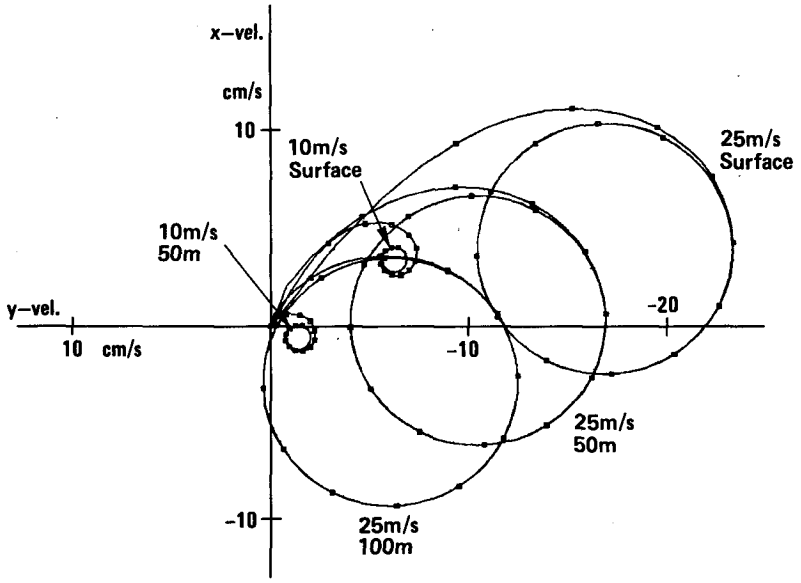

FIG. 9. Development in time of the quasi-Eulerian current for simulations 2 (wind speed 10 m s^{-1}) and 7 (wind speed 25 m s^{-1}).

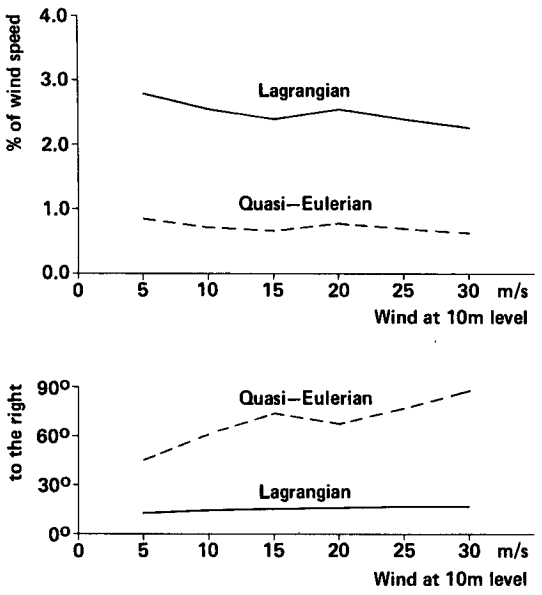

FIG. 10. Long-term average values of surface current as a percentage of wind speed, and direction of surface current with respect to the wind and wave direction. (Results of simulations 4, 2, 5, 6, 7, 8).

different directions are uncorrelated even if they have the same frequency.) The averaging interval needs to be long enough to eliminate low-frequency oscillations due to interference of wave components closely spaced in frequency (Chang, 1969).

As a consequence of the lack of correlation between wave components of different wavenumber, we can derive equations corresponding to (5.1) and (5.2) for a random wave field simply by summing or integrating the individual contributions due to the different wavenumber components in the directional wave spectrum, performing individual rotations of the coordinate axes (a, b) as necessary.

Low frequency oscillations due to interference of nearby wavenumber components are of interest in themselves: they will give rise to *Langmuir circulations* (LCs)—helical roll vortices, which occur in the near-surface layer of the ocean and other water bodies and which have axes nearly parallel with the wind and wave direction. Langmuir circulations give rise to zones of surface convergence and divergence, and contribute to near-surface mixing. The interference of wave components to produce LCs has been demonstrated in the case of a constant eddy viscosity by Craik and Leibovich (1976), N. E. Huang (1979) and Weber (1985). Using nonaveraged versions of (4.1)–(4.3), a theory of LCs in the presence of a vertically varying eddy viscosity can be developed.

c. *Spatial variation of the wave field*

The parameter d_s appears in the surface boundary condition (5.2) as a contribution to the factor $[d_0 + \frac{1}{2}(\chi - \chi_c) - (d_t + \frac{1}{2}d_s)]_{c=0}$, which in turn represents the rate at which the waves would grow as a result of external forces (in a reference frame moving with the group velocity) in the *absence* of dissipative effects. Thus, the surface boundary condition can be obtained, if we do not have direct measurements of the spatial variation of the wave field, by applying appropriate theories of wave growth based on field measurements of pressure fluctuations over wave crests, laboratory experiments, etc. (Hasselmann et al., 1973; Snyder et al., 1981; Mitsuyasu and Honda, 1982). The application of such wave growth theories is performed routinely in numerical wave models (e.g., see Komen et al., 1984). It should be noted that the surface boundary condition (5.2) is not affected by the nonlinear interaction of different wave components. Such interactions preserve total wave momentum, so that there is no resultant momentum excess or deficit to be compensated for at the surface.

d. *Evaluation of eddy viscosity profile*

The theory developed in this paper is self-consistent in the sense that the eddy viscosity parameterization of momentum transfer is used not only to relate shear stress and the rate of shear in the current, but also to control the dynamics of the surface gravity wave field. Thus, the eddy viscosity profile and the rates of wave dissipation are intimately related: as we have already stated, we assume that all wave dissipation processes are included within the eddy viscosity formulation. Hasselmann (1974) and Komen et al. (1984) have determined rates of wave dissipation as a function of frequency and global wave parameters from general theoretical considerations and from numerical experiments. Since longer-wavelength components penetrate deeper into the water column, their dissipation will be affected by the values of eddy viscosity at greater depths than shorter-wavelength components. This effect can be seen by examining the behavior of the dimensional version of (3.28), the exponential factor in the integral decaying more slowly with depth for longer-wavelength components. Thus, if we have an expression for the rate of wave dissipation as a function of frequency, we can estimate the eddy viscosity profile within the zone of wave influence. The eddy viscosity profile below the wave zone must, of course, be estimated by other means.

e. *Summary: applications*

It should thus be relatively straightforward to apply and extend the theory to the case of a random wave field, to incorporate the effect of spatial variations of the wave field, and to investigate more closely the near-surface eddy viscosity profile by considering frequency-dependent rates of wave dissipation. The most promising next step will be to combine the theory with the output from a numerical wave model, using the wave

model's input and dissipation source terms in the equation for the surface boundary condition.

7. Conclusion

This paper extends the Lagrangian coordinate perturbation theory treatment developed by Weber (1983a,b) and in J1 for wind and wave induced currents in a viscous rotating sea, to the case of a sea which has an eddy viscosity which is a function of the Lagrangian vertical coordinate. The main differences caused by the introduction of a vertically varying eddy viscosity are as follows:

(i) The surface gravity wave velocity field has a small rotational component within the water column [$A\chi(c)$], as well as near the surface boundary [$BM(c)$].

(ii) The rate of wave dissipation is a functional of the viscosity within the zone of wave influence [see (3.28)].

(iii) The differential equation which describes the evolution of the quasi-Eulerian current within the water column has an additional source term, locally proportional to the vertical gradient of the eddy viscosity. This source of momentum is balanced exactly by an additional term in the surface boundary condition, which represents the contribution to wave damping caused by the eddy viscosity within the water column being different from its surface value.

(iv) As would be expected, the $\nu\hat{W}^{(r)}_{\hat{c}\hat{c}}$ term in the equation for the evolution of the quasi-Eulerian current profile is replaced by $(\partial/\partial\hat{c})[\nu\hat{W}^{(r)}_{\hat{c}}]$.

The behavior of the quasi-Eulerian current depends on the net rate of wave growth, but is independent of the partition of the rate of wave energy input between horizontal and vertical cyclic surface stress variations.

Numerical simulations were performed with a constant wind stress and monochromatic wave field in the same direction, applied simultaneously at $\hat{t} = 0$. The eddy viscosity was assumed to be proportional to depth, using Madsen's (1977) relation, except for near the surface where it was modified to account empirically for the direct effects of breaking waves. Results for the Lagrangian mean current were in reasonable agreement with observations, given the crude nature of the wind and wave forcing which was used. The deviation of the current from the wind and wave direction was closer to observed drift current observations than the corresponding results for a constant eddy viscosity (Weber, 1983b). The results are, in fact, in agreement with those of Madsen's (1977) model below the zone of wave influence. Within the wave zone, agreement with Madsen's results is better for the Lagrangian mean rather than the Eulerian mean current.

It is straightforward to apply the theory to the case of a random seastate. A promising approach will be to couple it with the output from a numerical wave model, using as input data the wave model's input and dissipation source terms as well as the wind stress and the directional wave spectrum. We should also be able to use the frequency dependence of the dissipation source function to estimate the vertical variation of the eddy viscosity within the wave zone.

If a nonaveraged version of Eqs. (4.1)–(4.3) is used, the theory can be extended to investigate Langmuir circulations and other phenomena dependent on the interaction of wave components of the same frequency or of closely spaced frequencies, in the presence of a vertically varying eddy viscosity.

Acknowledgments. I thank my colleagues in the Oceanographic Center and in I.K.U. A/S for providing good quality computing facilities and a high standard of technical and other assistance. This work was partly supported by the Royal Norwegian Council for Scientific and Industrial Research.

REFERENCES

Barstow, S. F., 1981: Wave induced mass transport: theory and experiment. Ph.D. thesis, Heriot-Watt University, Edinburgh, 219 pp.

Bender, C. M., and S. A. Orszag, 1978: *Advanced Mathematical Methods for Scientists and Engineers.* McGraw-Hill, 593 pp.

Chang, M.-S., 1969: Mass transport in deep-water long-crested random gravity waves. *J. Geophys. Res.*, **74,** 1515–1536.

Craik, A. D. D., and S. Leibovich, 1976: A rational model for Langmuir circulations. *J. Fluid Mech.*, **73,** 401–426.

Davies, A. M., 1985a: Application of a sigma coordinate sea model to the calculation of wind-induced currents. *Contin. Shelf Res.*, **4,** 389–423.

——, 1985b: A three-dimensional modal model of wind induced flow in a sea region. *Progress in Oceanography,* Vol. 15, Pergamon, 71–128.

Dobroklonskiy, S. V., 1969: Drift currents in the sea with an exponentially decaying eddy viscosity coefficient. *Oceanology,* **9,** (English language edition) pp. 19–24.

Donelan, M. A., 1982: The dependence of the aerodynamic drag coefficient on wave parameters. *Preprint First Int. Conf. on Meteorology and Air/Sea Interaction of the Coastal Zone,* The Hague, Netherlands, Amer. Meteor. Soc., pp. 381–387.

Ekman, V. W., 1902: Om jordrotationens inverkan på vindströmmar i hafvet. *Nyt Magazin for Naturvidenskab,* **40**(1), 37–64.

——, 1905: On the influence of the earth's rotation on ocean-currents. *Ark. Mat. Astron. Fys.*, **2,** 1–53.

Gonella, J., 1971: A local study of inertial oscillations in the upper layers of the ocean. *Deep-Sea Res.*, **18,** 775–788.

Hasselmann, K., 1970: Wave-driven inertial oscillations. *Geophys. Fluid Dyn.*, **1,** 463–502.

——, 1974: On the spectral dissipation of ocean waves due to white-capping. *Bound. Layer Meteor.*, **6,** 107–127.

——, T. P. Barnett, E. Bouws, H. Carlson, D. E. Cartwright, K. Enke, J. A. Ewing, H. Gienapp, D. E. Hasselmann, P. Kruseman, A. Meerburg, P. Müller, D. J. Olbers, K. Richter, W. Sell and H. Walden, 1973: Measurements of wind-wave growth and swell decay during the Joint North Sea Wave Project (JONSWAP). *Dtsch. Hydrogr. Z.*, **A8**(12), 95 pp.

Huang, J. C., 1983: A review of the state-of-the-art of oil spill fate/behavior models. *Proc. 1983 Oil Spill Conf.*, San Antonio, Texas. American Petroleum Institute, pp. 313–322.

Huang, N. E., 1979: On surface drift currents in the ocean. *J. Fluid Mech.*, **91,** 191–208.

Jenkins, A. D., 1986: A theory for steady and variable wind and wave induced currents. *J. Phys. Oceanogr.*, **16,** 1370–1377.

Johns, B., 1970: On the mass transport induced by oscillatory flow in a turbulent boundary layer. *J. Fluid Mech.*, **43,** 177–185.

Kirwan, A. D., G. McNally, S. Pazan and R. Wert, 1979: Analysis of surface current response to wind. *J. Phys. Oceanogr.*, **9**, 401–412.

Komen, G. J., S. Hasselmann and K. Hasselmann, 1984: On the existence of a fully developed wind-sea spectrum. *J. Phys. Oceanogr.*, **14**, 1271–1285.

Lai, R. Y. S., and D. B. Rao, 1976: Wind drift currents in deep sea with variable eddy viscosity. *Arch. Meteor. Geophys. Bioklim.*, **A25**, 131–140.

Lamb, H., 1932: *Hydrodynamics*, 6th ed., Cambridge University Press, 738 pp.

Longuet-Higgins, M. S., 1953: Mass transport in water waves. *Philos. Trans. Roy. Soc. London*, **A245**, 535–581.

——, 1960: Mass transport in the boundary layer at a free oscillating surface. *J. Fluid Mech.*, **8**, 293–306.

——, 1970: Longshore currents generated by obliquely incident sea waves, 1. *J. Geophys. Res.*, **75**, 6778–6789.

Madsen, O. S., 1977: A realistic model of the wind-induced Ekman boundary layer. *J. Phys. Oceanogr.*, **7**, 248–255.

Miles, J. W., 1957: On the generation of surface waves by shear flows. *J. Fluid Mech.*, **3**, 185–204.

Mitsuyasu, H., and T. Honda, 1982: Wind-induced growth of water waves. *J. Fluid Mech.*, **123**, 425–442.

Pierson, W. J., 1962: Perturbation analysis of the Navier-Stokes equations in Lagrangian form with selected linear solutions. *J. Geophys. Res.*, **67**, 3151–3160.

Pollard, R. T., 1970: Surface waves with rotation: an exact solution. *J. Geophys. Res.*, **75**, 5895–5898.

——, 1973: Interpretation of near-surface current meter observations. *Deep-Sea Res.*, **20**, 261–268.

——, 1980: Properties of near-surface inertial oscillations. *J. Phys. Oceanogr.*, **10**, 385–398.

Snyder, R. L., F. W. Dobson, J. A. Elliott and R. B. Long, 1981: Array measurements of atmospheric pressure fluctuations above surface gravity waves. *J. Fluid Mech.*, **102**, 1–59.

Stokes, G. G., 1847: On the theory of oscillatory waves. *Trans. Cambridge Philos. Soc.*, **8**, 441–455.

Thorpe, S. A., 1984: On the determination of K_V in the near-surface ocean from acoustic measurements of bubbles. *J. Phys. Oceanogr.*, **14**, 855–863.

Ünlüata, Ü., and C. C. Mei, 1970: Mass transport in water waves. *J. Geophys. Res.*, **75**, 7611–7618.

Ursell, F., 1950: On the theoretical form of ocean swell on a rotating earth. *Mon. Not. Roy. Astron. Soc.*, (Geophys. Suppl.), **6**, 1–8.

Weber, J. E., 1983a: Attenuated wave-induced drift in a viscous rotating ocean. *J. Fluid Mech.*, **137**, 115–129.

——, 1983b: Steady wind- and wave-induced currents in the open ocean. *J. Phys. Oceanogr.*, **13**, 524–530.

——, 1985: Friction-induced roll motion in short-crested surface gravity waves. *J. Phys. Oceanogr.*, **15**, 936–942.

——, 1987: Eulerian versus Lagrangian approach to wave-drift in a rotating ocean. *Göteborgs Kungliga Vetenskaps-og Vitterhetssamhälle: Acta, Ser. Geofys.*, **4** (in press).